


# Biochemical and functional characterization of the p.A165T missense variant of mitochondrial amidoxime-reducing component 1

Received for publication, February 28, 2024, and in revised form, April 25, 2024. Published, Papers in Press, May 7, 2024.

<https://doi.org/10.1016/j.jbc.2024.107353>

Wangfang Hou<sup>1</sup> , Christian Watson<sup>1</sup>, Ted Cecconie<sup>2</sup>, Menaka N. Bolaki<sup>3</sup>, Jennifer J. Brady<sup>3</sup>, Quinn Lu<sup>1</sup>, Gregory J. Gatto, Jr.<sup>1,\*</sup>, and Tovah A. Day<sup>4</sup>

From the <sup>1</sup>Respiratory and Immunology Biology Unit, and <sup>2</sup>MEDDesign-NCE-MD SPMB US, GlaxoSmithKline, Collegeville, Pennsylvania, USA; <sup>3</sup>23andMe Therapeutics, Sunnyvale, California, USA; <sup>4</sup>Department of Biology, Northeastern University, Boston, Massachusetts, USA

Reviewed by members of the JBC Editorial Board. Edited by George DeMartino

Recent genome-wide association studies have identified a missense variant p.A165T in mitochondrial amidoxime-reducing component 1 (mARC1) that is strongly associated with protection from all-cause cirrhosis and improved prognosis in nonalcoholic steatohepatitis. The precise mechanism of this protective effect is unknown. Substitution of alanine 165 with threonine is predicted to affect mARC1 protein stability and to have deleterious effects on its function. To investigate the mechanism, we have generated a knock-in mutant mARC1 A165T and a catalytically dead mutant C273A (as a control) in human hepatoma HepG2 cells, enabling characterization of protein subcellular distribution, stability, and biochemical functions of the mARC1 mutant protein expressed from its endogenous locus. Compared to WT mARC1, we found that the A165T mutant exhibits significant mislocalization outside of its traditional location anchored in the mitochondrial outer membrane and reduces protein stability, resulting in lower basal levels. We evaluated the involvement of the ubiquitin proteasome system in mARC1 A165T degradation and observed increased ubiquitination and faster degradation of the A165T variant. In addition, we have shown that HepG2 cells carrying the *MTARC1* p.A165T variant exhibit lower N-reductive activity on exogenously added amidoxime substrates *in vitro*. The data from these biochemical and functional assays suggest a mechanism by which the *MTARC1* p.A165T variant abrogates enzyme function which may contribute to its protective effect in liver disease.

Nonalcoholic fatty liver disease (NAFLD) is a major cause of chronic liver disease. NAFLD affects over 64 million people in the United States and approximately 2 billion people worldwide (1, 2). About 10% of NAFLD patients progress to the most serious form, nonalcoholic

steatohepatitis (NASH). Cirrhosis, a severe complication of NASH and other chronic liver diseases, ranks as the 11th leading cause of death globally. It accounts for ~35,000 deaths annually in the US and represents a major public health burden (3–7). Despite this, there are currently no FDA-approved therapies for NASH (8).

Genome-wide association studies (GWAS) are a powerful tool to uncover associations between genetic variants and risk of disease; recently, they have also become an important strategy to identify new therapeutic targets (9, 10). Several recent studies applied GWAS to NASH and identified the missense variant p.A165T of the mitochondrial amidoxime-reducing component 1 (mARC1, encoded by the *MTARC1* gene) as protective from both alcoholic and nonalcoholic cirrhosis (1, 10, 11). It was found that *MTARC1* p.A165T changed lipid profile. Carriers with A165T showed higher level of hepatic polyunsaturated phosphatidylcholines than carriers with WT (12, 13). p.A165T has also been associated with lower liver enzymes, lower total cholesterol level (1, 10), reduced severity of NAFLD, and reduced liver-related mortality (1, 12). A subsequent study showed that *MTARC1* p.A165T variant was implicated in downregulation of the hepatic fibrotic pathway and associated with a lower grade of hepatic steatosis in children with NAFLD (13).

The mARC1 protein is one of the four molybdenum (Mo)-containing enzymes in the human genome (14). It localizes to the outer mitochondrial membrane and is predominantly expressed in liver and adipose tissue (15, 16). The C-terminal domain is exposed to the cytosol where it binds to a Mo cofactor (Moco) and functions as the catalytic core. The N-terminal domain contains a mitochondrial targeting sequence and a hydrophobic domain which anchors the protein on the outer mitochondrial membrane (15). mARC1 forms a complex with cytochrome *b*<sub>5</sub> reductase 3 (CYB5R3) and cytochrome *b*<sub>5</sub> type B (CYB5B), from which Moco receives electrons from NADH to enable mARC1 to reduce a large variety of N-oxygenated substrates including nitrite, N-hydroxylated nucleobases, amidoxime prodrugs, and physiological substrate *N*<sup>ω</sup>-hydroxy-L-arginine (NOHA) (17–22). Based on its enzymatic activity, mARC1 is hypothesized to play roles in cellular detoxification, L-arginine metabolism, nitric oxide biosynthesis,

\* For correspondence: Gregory J. Gatto, [greg.j.gatto@gsk.com](mailto:greg.j.gatto@gsk.com).

Present addresses for: Menaka N. Bolaki, Novartis Institutes for BioMedical Research (NIBR) San Diego, 10675 John Jay Hopkins Drive, San Diego, CA 92121 USA; Jennifer J. Brady: Variant Bio, 1150 Eastlake Ave E Suite 1000, Seattle, WA 98109 USA.

## Characterization of mARC1 p.A165T variant

and drug metabolism (20, 23, 24). Nitric oxide affects mitochondrial biogenesis and inhibits mitochondrial respiration, thereby influencing mitochondrial functions both physiologically and pathologically (25–28). Mitochondrial dysfunction leads to increased formation of reactive oxygen species and lipid peroxidation, which both contribute to NASH (29). These clinical observations, coupled with the GWAS finding (1, 10, 11), strongly suggest a role for mARC1 in NASH; however, the mechanistic details remain poorly understood.

A total of 27 nonsynonymous single nucleotide polymorphisms have been described for *MTARC1* (30). Among these, c.493A>G (rs2642438, resulting in p.A165T) has a minor allele frequency of 0.25 in the human population (31). *In silico* modeling predicted that *MTARC1* p.A165T variant would have lower stability and altered Mo binding (13). Mo binding is critical for mARC1 enzymatic function (32) and mutation of a highly conserved Mo-binding residue cysteine 273 to alanine completely abolishes the function of the protein (32, 33). However, purified, recombinant mARC1 A165T exhibited similar kinetic parameters to WT when reducing benzamidoxime (BAO) (30) and sulfamethoxazole hydroxylamine (17), two N-hydroxylated substrates. These observations suggest that A165T does not abrogate *in vitro* binding of Mo (30). Despite the lack of difference in recombinant enzyme turnover, GWAS of *MTARC1* p.A165T shows remarkably broad protection from liver fibrosis, steatosis, and cirrhosis and a benefit in NASH. This protective effect of p.A165T is very similar to a rare nonsense mutation p.R200Ter, a loss-of-function variant which completely lacks the catalytic domain at the C terminus of the protein (10). All these data indicate that elucidation of a protective mechanism in a cellular context will yield important insights into this modulator of liver diseases. Owing to the long half-life of mARC1 (~12 days) (34) in primary human hepatocytes and the limitations of long-term culture of primary human hepatocytes (35), we chose genome-edited HepG2 cells as the model for our study. Our exploration provides biochemical

and functional explanations for the protection effect of this variant using a cellular model.

## Results

### mARC1 A165T protein is mislocalized in HepG2 cells

mARC1 is a mitochondrial protein localized to the outer mitochondrial membrane (15). To investigate whether single amino acid changes in mARC1 variants affected protein subcellular localization, we applied high content imaging assay to study the subcellular localization of mARC1 in HepG2 cells. mARC1 protein and mitochondria were both imaged, and colocalization of the protein with mitochondria was analyzed for >6000 cells. In cells expressing the A165T variant, more diffuse staining of mARC1 protein was observed when compared to WT and C273A, a catalytically dead mutant (Fig. 1A). Colocalization analysis of mARC1 staining and mitochondrial staining revealed that the A165T variant colocalizes with mitochondria significantly less than WT (Fig. 1A). This was quantitated as FITC intensity of mARC1 protein for mitochondrial puncta for an average from >6000 cells. The average corrected FITC spot intensity of mitochondrial puncta of A165T was significantly lower than that of WT or C273A (Fig. 1B). The ratio of average FITC intensity of cytoplasm to mitochondria for A165T was significantly higher than that of WT or C273A (Fig. 1C), indicating higher mislocalization of A165T than WT or C273A.

### A165T destabilizes mARC1

To further characterize the effect of A165T on mARC1, we examined the endogenous level of mARC1 expression in CRISPR-edited HepG2 cells expressing different variants. mRNA and protein level of mARC1 were determined for the three HepG2 cell lines carrying different *MTARC1* genotypes including WT, A165T, and C273A. There was no significant difference in the levels of mRNA among the three genotypes (Fig. 2A). The negative control, HepG2 mARC1 KO cells

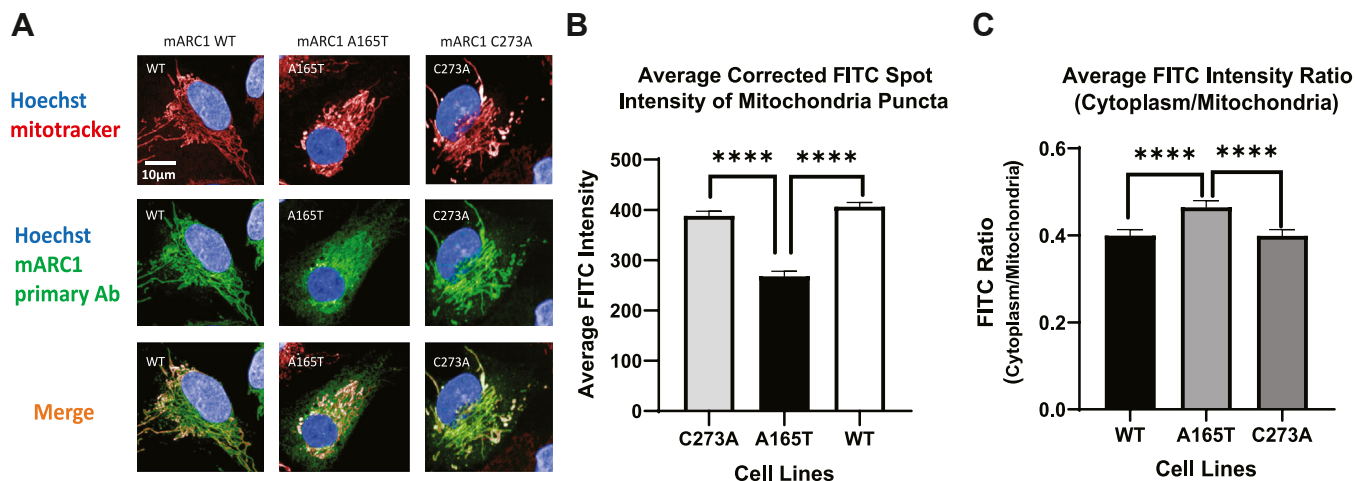


**Figure 1. Subcellular localization of mARC1 variants and comparison of their level on mitochondria.** A, imaging data for colocalization of mARC1 with mitochondria. B, average-corrected FITC (mARC1) spot intensity of mitochondria puncta. C, ratio of average FITC intensity of cytoplasm to mitochondria. Data represents an average from six wells from which >1000 cells were analyzed from each well (\*\*\*\*  $p < 0.0001$ ). mARC1, mitochondrial amidoxime-reducing component 1.

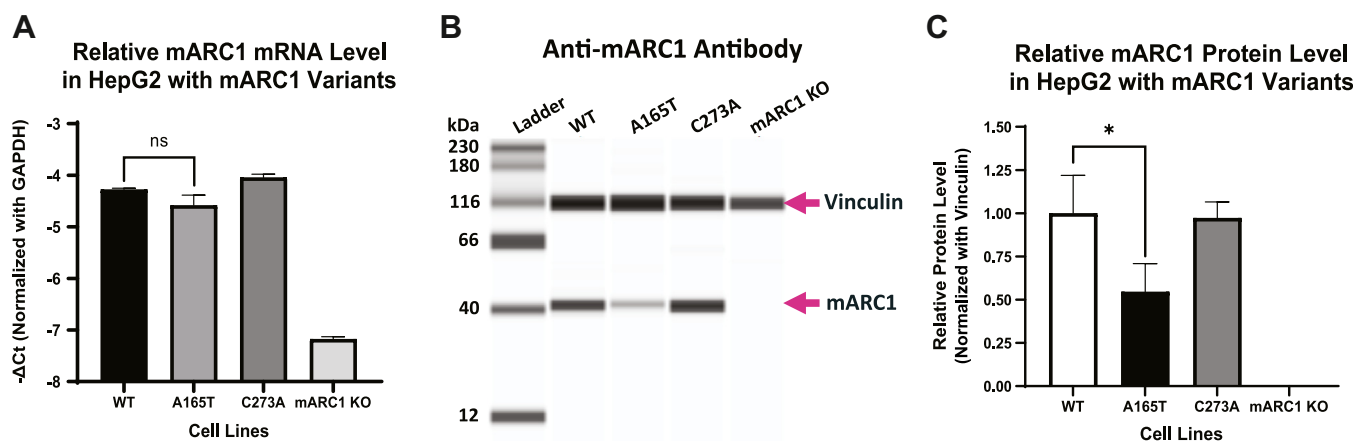


**Figure 2. mRNA and protein expression level of mARC1 in HepG2 cells with different genotypes.** A, mRNA level in cells of the indicated genotype. B, Jess immunoblotting analysis for protein expression in the three HepG2 cell lines with mARC1 WT, A165T, and C273A genotype. C, relative mARC1 protein expression level after normalization (data was first normalized with vinculin level in the same cell line and then normalized with the relative protein level in WT cells) (\*  $p < 0.05$ ). mARC1, mitochondrial amidoxime-reducing component 1.

deficient in mARC1, exhibited dramatic (>90%) loss of mARC1 mRNA relative to WT (Fig. 2A).

In contrast, genotype-dependent changes in mARC1 protein levels were observed. Significantly lower mARC1 protein levels ( $\sim 54 \pm 16\%$ ) were detected in the A165T cells relative to WT (Fig. 2, B and C). mARC1 KO cells did not express mARC1 protein, verifying the specificity of the immunoblotting analysis. These results indicate that A165T leads to lower levels of mARC1 protein (Fig. 2, B and C).

#### Ectopically expressed mARC1 A165T exhibits reduced stability in double KO cells

Several studies reported that recombinant mARC1 A165T has similar N-reductive activity to WT in a cell-free assay (17, 30). This finding may indicate that WT and A165T have similar activities and stabilities outside of a cellular environment. However, our study demonstrates that mARC1 A165T expressed from its endogenous promoter is less stable than WT and C273A in HepG2 cells. To rule out the possible effect on mARC1 level caused by other factors in HepG2 cell lines carrying different mARC1 genotypes, ectopically expressed mARC1 variants in the same HepG2 cell line with knockout of both mARC1 and mARC2 (double knockout, dKO) were examined using the BacMam system. While no mARC1 protein was detected in the dKO cells, ectopically expressed mARC1 protein was detected for all genotypes including WT, A165T, or C273A. Endogenous mARC1 in WT HepG2 cells served as a positive control and a measure of endogenous expression levels. Notably, the level of mARC1 protein was much lower in the cells expressing A165T variant than cells expressing WT or C273A (Fig. 3A). A similar expression pattern was observed in BacMam expressing mARC1-GFP fusion proteins: A165T-GFP showed much lower expression than either WT-GFP or C273A-GFP (Fig. 3B). These results suggest that A165T decreases the stability of ectopic mARC1 protein.

#### mARC1 A165T does not affect CYB5B and CYB5R3 expression

The N-reductive activity of mARC1 requires the presence of two additional proteins localized to the outer mitochondrial membrane, cytochrome  $b_5$  type B and NADH-cytochrome  $b_5$  reductase (19, 21, 22). In our study, we examined protein expression levels of CYB5B and CYB5R3 in the genome-edited HepG2 cell lines expressing the three mARC1 variants: WT, A165T, or C273A. We found high levels of CYB5B and CYB5R3 protein were expressed in all three cell lines that were not significantly different between genotypes (Fig. 4, A and B). These data also suggest that the mARC1 variants do not significantly impact overall mitochondrial number or stability.

#### Endogenous mARC1 A165T is degraded more rapidly than mARC1 WT

HepG2 cells expressing mARC1 A165T, either endogenously or ectopically, exhibit lower levels of mARC1 protein than cells expressing either WT or C273A. To test whether lower mARC1 A165T levels are due to more rapid protein degradation, HepG2 cells with different mARC1 genotypes (WT, A165T, and C273A) were treated with two different concentrations (10  $\mu\text{M}$  and 20  $\mu\text{M}$ ) of cycloheximide, an inhibitor of protein translation, for 8 h, and mARC1 protein levels were measured. A165T mARC1 protein levels were decreased relative to vehicle at both concentrations of cycloheximide. In contrast, WT and C273A mARC1 protein levels were minimally affected by cycloheximide treatment (Fig. 5).

#### Degradation of mARC1 A165T occurs through the ubiquitin-proteasome pathway

To determine whether the ubiquitin-proteasome system is responsible for the rapid degradation of mARC1 A165T, we examined ubiquitination of C-terminal Flag-tagged mARC1 WT, A165T, or C273A expressed in HepG2 dKO cells via BacMam transduction. The cells were treated sequentially with

## Characterization of mARC1 p.A165T variant

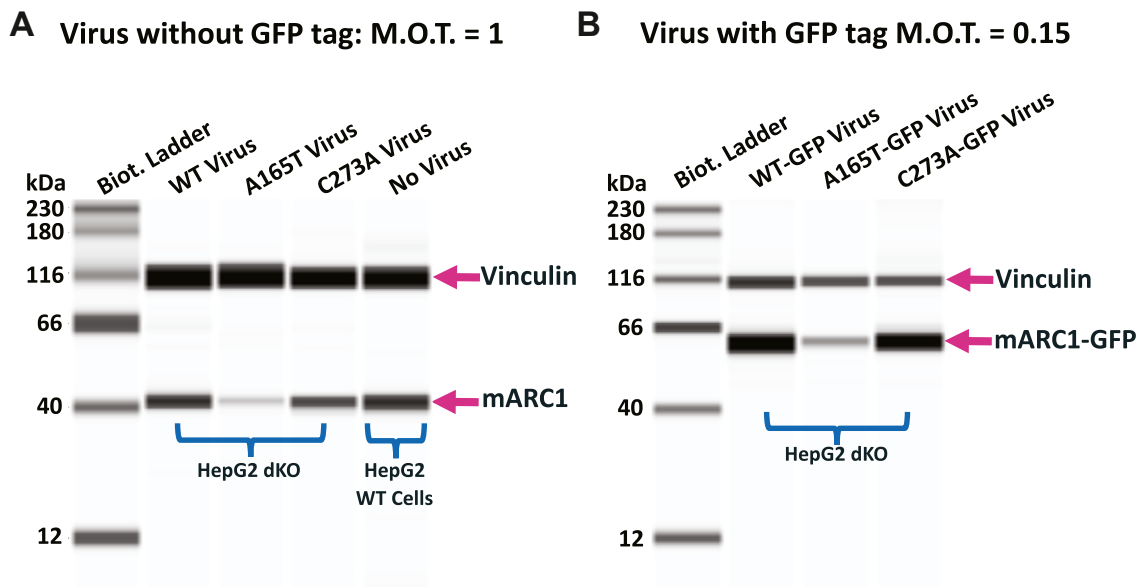


**Figure 3. mARC1 protein level in HepG2 dKO cells transduced with BacMam virus expressing mARC1 variants WT, A165T, or C273A w/o C-term GFP tag.** A, mARC1 protein expression in HepG2 dKO cells transduced with BacMam virus expressing mARC1 variants without GFP tag. B, mARC1 protein expression in HepG2 dKO cells transduced with BacMam virus expressing mARC1 variants with GFP tag. mARC1, mitochondrial amidoxime-reducing component 1.

cycloheximide and MG-132, an inhibitor of the proteasome. Immunoprecipitation (IP) of mARC1-Flag demonstrated that basal ubiquitination of mARC1 was significantly elevated in A165T-expressing cells relative to WT or C273A (Fig. 6, A and C), even though A165T protein level is much lower than WT (Fig. 6B). When the ubiquitinated mARC1 was normalized with the nonubiquitinated mARC1 protein immunoprecipitated (IP'd), ubiquitination of A165T was ~4 times higher than that of WT or C273A. Upon treatment with cycloheximide, both the ubiquitination signal and protein IP'd of A165T was reduced to much lower levels (Fig. 6, A–C). Upon the treatment of MG-132, both the ubiquitination signal and protein IP'd of A165T increased (Fig. 6, A–C). Under all conditions, normalized

ubiquitination signal of A165T was higher than WT or C273A, while WT and C273A showed similar levels (Fig. 6C). These results underscore the importance of the proteasome in the degradation of A165T.

### mARC1 A165T has reduced N-reductive activity in HepG2 cells

The mARC1 enzyme contributes to *in vivo* reduction of N-hydroxylated substrates (19, 21). Many studies have demonstrated this reductive function of mARC1 using recombinant proteins (17, 20, 23, 30, 36). We designed a cellular substrate turnover assay to evaluate the N-reductive activity of endogenous mARC1 variants in HepG2 cells using a model substrate BAO and a putative physiological substrate of

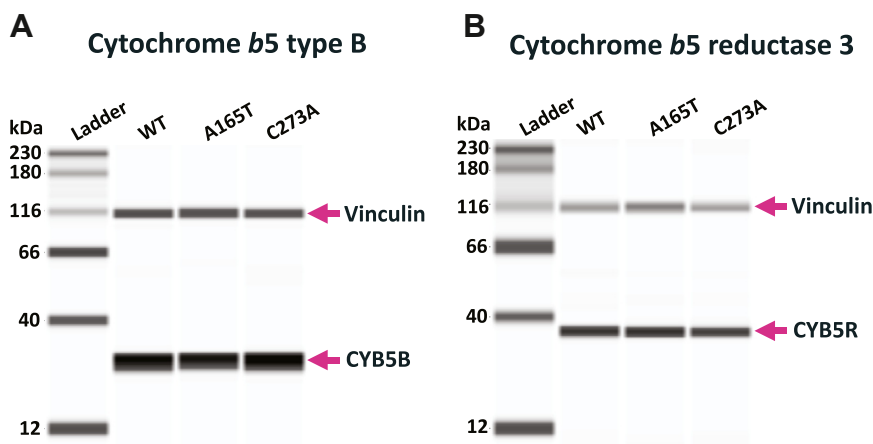


**Figure 4. Cytochrome b<sub>5</sub> type B and cytochrome b<sub>5</sub> reductase 3 protein expression in HepG2 cells with different mARC1 genotypes: WT, A165T, or C273A.** A, expression of cytochrome b<sub>5</sub> type B protein in the three HepG2 cell lines. B, expression of cytochrome b<sub>5</sub> reductase 3 protein in the three HepG2 cell lines. mARC1, mitochondrial amidoxime-reducing component 1.

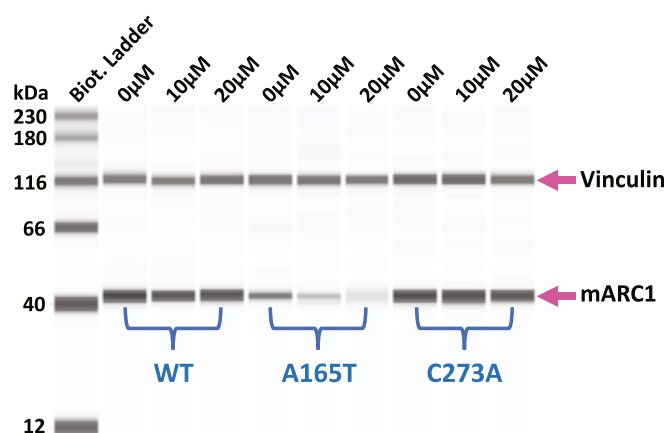


**Figure 5. Protein stability analysis for mARC1 WT, A165T, and C273A.** HepG2 cell lines with three different *MTARC1* genotypes WT, A165T, or C273A were treated with 0  $\mu$ M (DMSO only), 10  $\mu$ M, and 20  $\mu$ M of cycloheximide for 8 h. mARC1 protein expression level was examined in those cell lines using ProteinSimple/Jess system. A representative image of four repeats of Simple Western results is shown here. (The loading amount of each lane was normalized to vinculin levels to adjust for a small change in vinculin levels with cycloheximide (data not shown)). mARC1, mitochondrial amidoxime-reducing component 1.

mARC1 NOHA. We used a flow injection analysis RapidFire-Triple Quadrupole-Mass Spectrometric analysis method (RF-QQQ-MS) to measure the amount of benzamide (BA) or L-arginine, the products of BAO and NOHA reduction, respectively, produced by cells and released into the tissue culture media. While HepG2 cells expressing WT mARC1 showed the highest efficiency in reducing both substrates, cells expressing the A165T variant exhibited only  $\sim$ 70% of WT reduction capacity in reducing BAO to BA (Fig. 7A) and  $\sim$ 50% of WT reduction capacity in reducing NOHA to L-arginine (Fig. 7B). This is consistent with the relatively lower protein levels of A165T in this cell line. As expected, cells expressing the catalytically dead mutant C273A had the lowest reduction capacity, exhibiting  $\sim$ 20% (BAO to BA, Fig. 7A) or 13% (NOHA to L-arginine, Fig. 7B) of WT capacity, which is likely due to the expression of mARC2 protein in these cells. A HepG2 cell line expressing the C273A variant with mARC2 KO showed no reductive activity for either substrate (Fig. S1).

## Discussion and conclusion

NAFLD/NASH is a multifactorial disease, and recent GWAS have shown that genetic variations play a crucial role in disease susceptibility, development, and severity (1, 10, 13, 37–40). Some genetic variants such as *PNPLA3* rs738409C>G (I148M) and *TM6SF2* rs58542926C>T (E167K) appear to increase the risk of NAFLD/NASH, while other genetic variants offer protection against the disease. *MTARC1* rs2642438G>A (A165T) is one of the recently reported variants associated with protection from NASH (1, 10, 13, 37, 40). Based on the fact that *MTARC1* p.A165T shows a similar lipid phenotype and protective effect from cirrhosis as the loss of function variant p.R200Ter, it has been surmised that a loss of function induced by A165T may contribute to its association with a decreased risk in NAFLD/NASH (10). However, the underlying mechanism that links *MTARC1* p.A165T variant to its beneficial effect in liver disease remains unclear, especially since it has been reported that recombinant mARC1 carrying this variant appears to have a similar specific activity to the WT protein (17, 30). Indeed, further characterization of mARC1 A165T protein in hepatocytes, including biochemical and functional properties of the protein, is imperative to obtain a clearer understanding of the biological connection between mARC1 and NASH and provide insight for the development of drug therapies for cirrhosis.

Using CRISPR/Cas9 genome editing, we generated isogenic HepG2 cell lines that express different variants of mARC1, including A165T and C273A. No significant difference in levels of mRNA was found between A165T and WT. Our results are consistent with the published result that mRNA expression level was not significantly affected by *MTARC1* p.A165T in liver tissue samples from patients with NAFLD (11, 41). However, the level of protein expression was significantly affected by genotype. mARC1 A165T showed  $\sim$ 50% reduction of protein expression levels when compared to WT protein in HepG2 cells. Moreover, expression of mARC1 A165T in HepG2 cells by BacMam viral transduction at low multiplicity of transduction also showed dramatically less A165T protein compared to WT and C273A. Both experiments demonstrate that the impact of A165T on mARC1 levels occurs at the protein level.

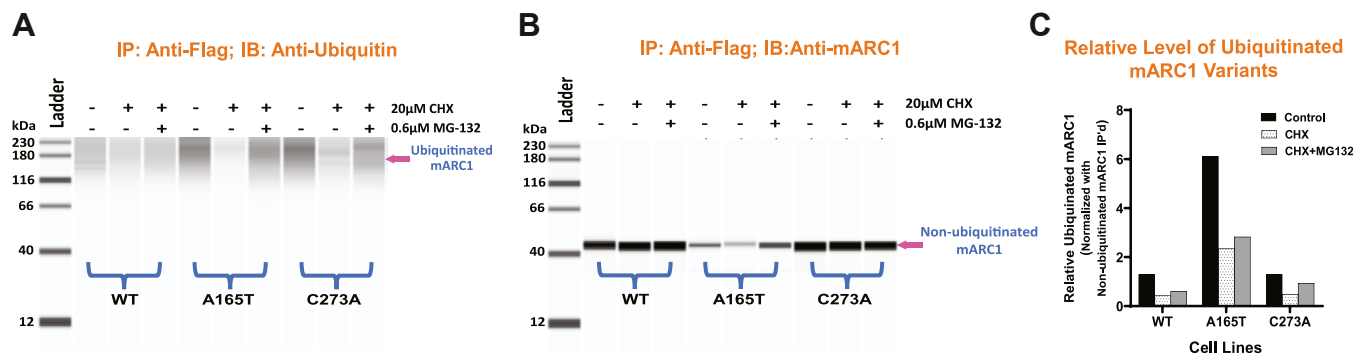


**Figure 6. Degradation of mARC1 A165T by ubiquitin proteasome pathway.** Jess immunoblotting analysis for mARC1 protein immunoprecipitated showing ubiquitination patterns and protein level under different conditions for the three mARC1 variants. A, protein detected using anti-ubiquitin antibody. B, protein detected using anti-mARC1 antibody. C, relative level of ubiquitinated mARC1 variants normalized with non-ubiquitinated mARC1 protein IP'd (protein bands in A and B were quantitated by ImageJ). mARC1, mitochondrial amidoxime-reducing component 1.

## Characterization of mARC1 p.A165T variant

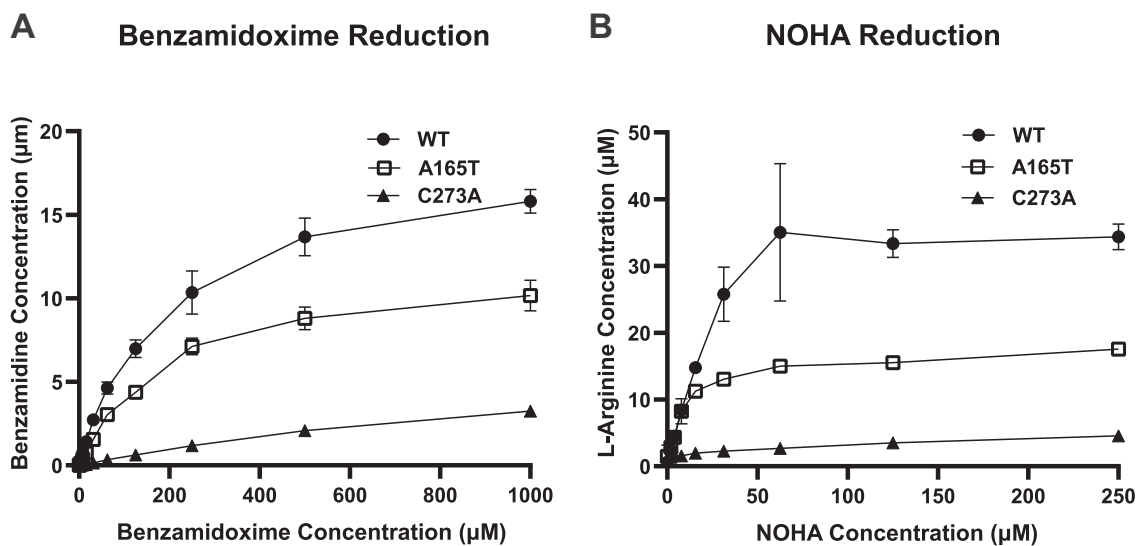


**Figure 7. N-reductive activity in HepG2 cells with different mARC1 genotype: WT, A165T, or C273A.** A, benzamidine (BA) generated by the three cell lines in response to the treatment with various concentrations of BAO. B, L-Arginine generated by the three cell lines in response to the treatment with various concentrations of NOHA. NOHA, N<sup>ω</sup>-hydroxy-L-arginine.

We also observed that the expression levels of CYB5B and CYB5R3, two outer mitochondrial membrane proteins that are required for mARC1 activity, were not significantly affected by the expression of the A165T variant of mARC1. This indicates that genotype of mARC1 does not impact mitochondrial number or stability. Further, the concentrations of CYB5B and CYB5R3 are not rate-limiting factors for the N-reductive activity of mARC1 in the setting of A165T (32). Nevertheless, while our results indicate that the A165T variant does not impact CYB5B and CYB5R3 protein levels, there remains the possibility, beyond the scope of this work, that this variant impacts the efficiency of electron transfer within the reductase complex.

We then further explored the underlying mechanism that explains the observed lower protein levels of A165T variant. Our findings revealed that mARC1 A165T exhibited mislocalization from the outer mitochondrial membrane to cytosol. mARC1 to the outer mitochondrial membrane allows it to function together with the other two components cytochrome *b*<sub>5</sub> and cytochrome *b*<sub>5</sub> reductase to form an intact N-reductive system in the cells (15, 42). Subcellular localization of mARC1 is mediated by its N-terminal targeting signal (aa. 1-20) and transmembrane domain (aa. 21-40) (15). The C-terminal catalytic Moco-containing domain (aa. 41-337) is exposed to the cytosol (15). Evidence from mARC1 crystal structures and published data which show similar Mo content among different recombinant mARC1 variants collectively indicate that residue 165 is not involved in Moco binding (30, 33).

We posit that the alteration of a single amino acid from a hydrophobic to polar amino acid is able to change the anchoring of mARC1 on the outer mitochondrial membrane and cause its mislocalization, even in the absence of significant protein secondary structure changes (43). A recent crystal structure study of mARC1 A165T showed that there were alternate conformations of Thr165, even though no difference in protein folding

and thermal stability was found between A165T and WT (44). Our observation that mARC1 A165T is mislocalized suggests that replacement of Ala by Thr at this position may disrupt mitochondrial anchoring of the protein. Even though this amino acid is not in the transmembrane domain, it could affect interaction with other proteins that might be involved in mARC1 mitochondrial membrane targeting and binding (45). Proteins localized on the mitochondrial outer membrane have been found to be degraded by the ubiquitin-proteasome pathway (46, 47). The proteins are polyubiquitinated for degradation in cytosol after they are extracted from the membrane (48, 49). When mARC1 protein is detached from the mitochondrial membrane and released into cytosol, it may be more available for polyubiquitination and degradation by cytosolic ubiquitin-proteasome pathway. In our study, by blocking protein translation, we found that A165T was more rapidly degraded than the WT and C273A protein. Our study further demonstrates that the A165T protein showed greater ubiquitination levels than WT in HepG2 cells. In addition, ubiquitinated A165T was degraded faster than ubiquitinated WT, suggesting greater access (*i.e.* enhanced recognition or entry) to the proteasome. Our data suggest that correct protein localization of mARC1 on the mitochondrial membrane is crucial for maintaining mARC1 protein stability in cells.

In addition to reduced protein levels, mislocalization of A165T can result in the loss of function of mARC1 since it must interact with cytochrome *b*<sub>5</sub> and cytochrome *b*<sub>5</sub> reductase on the outer mitochondrial membrane for its N-reductive activity (22). Hudert *et al.* identified a protective effect for children with NAFLD carrying the p.A165T variant, but they observed no change in the level of protein expression of A165T compared to WT (13). By contrast, Smagris, *et al.* observed a ~60% reduction of mARC1 protein in liver samples from A165T carriers compared to WT (41). This apparent discrepancy may reflect a loss-of-function phenotype that is

primarily driven by the subcellular mislocalization of A165T without a significant lowering of protein levels in the NAFLD children-derived biopsy samples reported by Hudert, *et al.* Further studies on the expression levels and subcellular localization of *mARC1* and its variants in samples from human patients are clearly warranted.

After establishing the effect of A165T on *mARC1* protein stability and level in cells, we assessed its effect on protein functionality in intact cells through a cell-based substrate turnover assay. In HepG2 cells with the A165T genotype, N-reductive activity for both BAO and NOHA was significantly reduced when compared with WT cells. Previous studies have shown that recombinant *mARC1* A165T and *mARC1* WT have similar Moco-binding efficiency (30) and similar kinetic parameters in reducing sulfamethoxazole hydroxylamine and BAO (17, 30). These data indicate that A165T does not affect N-reductivity of recombinantly expressed *mARC1* protein outside of a cellular environment. Taking into account observations from our data, we propose that the decrease in net substrate turnover by A165T in HepG2 cells is due to improperly localized A165T *mARC1* protein that separates it from its catalytically essential electron transfer partners and simultaneously reduces the total amount of protein.

As expected, the C273A mutation abolished about 80% of N-reductive capability of HepG2 cells. This is consistent with the reported loss of Moco binding by this variant. The residual activity in these cells is likely due to endogenous *mARC2* protein, a paralog of *mARC1* expressed in these cells which shares similar substrates. The HepG2 cell line expressing the C273A variant with *mARC2* KO showed negligible reductive activity, similar to HepG2 dKO cells (Fig. S1). This is further supported by a rescue experiment in which C273A overexpression was unable to rescue any of the N-reductive activities of the HepG2 dKO cells (data not shown).

Consistent with our findings, three papers published while this manuscript was in review also found that p.A165T decreased stability of *mARC1* protein overexpressed in cell lines and mice (41, 50, 51). In addition, Dutta *et al.* similarly reported that overexpressed *mARC1*-A165T is primarily degraded *via* the proteasome pathway. In this study, we extend

their work by using genome-edited cell lines to demonstrate that endogenously expressed *mARC1*-A165T is also significantly reduced relative to the WT protein. Furthermore, using these edited cell lines and a cellular *mARC1* activity assay, we are able to show that the reduction in protein level driven by this variant displays a concomitant reduction in enzymatic activity (Figs. 2 and 7). Finally, high content imaging reveals that endogenously expressed *mARC1* A165T is, in part, mislocalized from the mitochondria (Fig. 1), which may provide an explanation for its apparent instability.

In conclusion, our findings reported here provide biochemical and functional evidence in HepG2 cells supporting the recent GWAS discovery that the A165T variant confers a protective effect on NASH by inducing a functional deficiency of *mARC1*. Our characterization of subcellular localization and protein stability of *mARC1* variants in HepG2 cells support that functional deficiency of the A165T variant in cells is attributable to mislocalization of the variant, which abrogates the interaction of the protein with cytochrome *b<sub>5</sub>* and cytochrome *b<sub>5</sub>* reductase for its function. Further, mislocalization of A165T enhanced degradation of the protein by the ubiquitin-proteasome pathway resulting in a decreased protein abundance (Fig. 8). The results from our study provide a possible explanation why *MTARC1* p.A165T shows similar protective effects from liver disease as the loss-of-function variant p.R200Ter. Together with the fact that the *mARC1* protein is involved in lipid metabolism and the hepatic fibrotic pathway, our study supports the therapeutic hypothesis that antagonism of *mARC1* protein may be a useful method in treating NAFLD and NASH.

## Experimental procedures

### BacMam virus generation for expressing various *mARC1* constructs

Sequence for human *MTARC1* WT, *MTARC1* p.A165T, *MTARC1* p.C273A (reference: NM\_022746.4) with or without GFP tag were synthesized and cloned into pHTBV1mcs3, a second generation of BacMam vector (52). (–) control virus was made from pHTBV1mcs3 empty vector. BacMam virus expressing the constructs was then generated *via* the Bac-to-

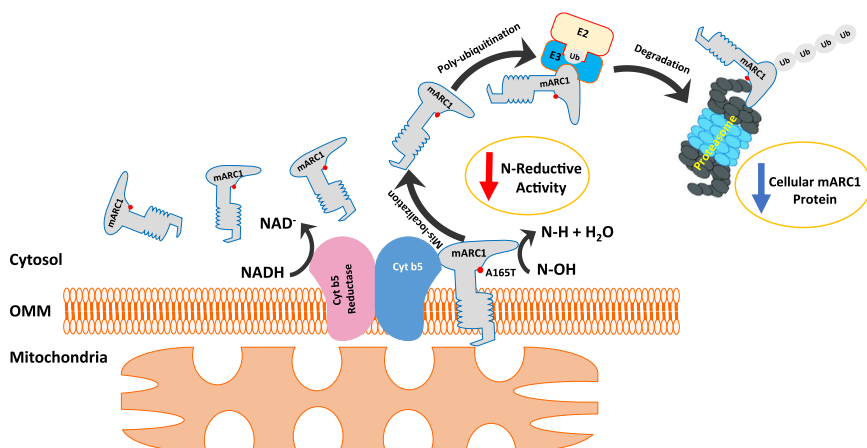


**Figure 8. Mislocalization causes fast degradation of *mARC1* A165T by ubiquitin/proteasome pathway.** *mARC1*, mitochondrial amidoxime-reducing component 1.

## Characterization of *mARC1* p.A165T variant

Bac system. Both plasmid cloning and BacMam virus generation were done by GenScript.

### HepG2 cell line culture

HepG2 (ATCC) cells were routinely cultured in EMEM + 10% fetal bovine serum (Thermo Fisher Scientific) culture medium and split twice every week.

### HepG2 (*MTARC1*<sup>-/-</sup>, *MTARC2*<sup>-/-</sup>) dKO cell line generation

The guide RNAs (gRNAs) targeting *MTARC1* and *MTARC2* were ordered from Integrated DNA Technologies (IDT). The sequence of gRNA used for *MTARC1* is GAAGCTGGT-TATCCACTGGG and the sequence of gRNA used for *MTARC2* is GTAGATCCAGAGCTTCGCCA. Alt-R *Staphylococcus pyogenes* Cas9 Nuclease V3 and Alt-R CRISPR-Cas9 tracrRNA were also ordered from IDT. Cas9 gRNA and tracrRNA was first incubated together in tubes to form ribonucleoprotein (RNP) complex. The RNP was then transfected into HepG2 using the 4D Nucleofector system for HepG2 (Lonza). To generate HepG2 dKO cells, HepG2 were first transfected with RNP for *MTARC2* and recovered for 3 days. They were then transfected once again with RNP for *MTARC1*. Three days after the second transfection, cells were plated out into 96-well plates at a density of one cell/well for generating single clonal cell lines. After cells grew to full confluence in each well, the cell lines were screened for *MTARC1* and *MTARC2* genotype *via* PCR followed by Sanger sequencing. The sequencing results were analyzed using the Inference of CRISPR Edits (ICE) online analysis tool on the Synthego website. Cell lines with KO genotype (frameshift) for both *MTARC1* and *MTARC2* were expanded and pooled together with same cell number from each clonal line. A total of 26 individual clonal cell lines were pooled together for the final dKO cell line used in this study.

### Generation of pooled HepG2 clonal cell lines with *MTARC1* genotype: WT, A165T, or C273A

To generate *MTARC1* p.A165T and C273A knock-in (KI) cell lines, RNP targeting *MTARC1* genomic DNA sequence around A165 or C273 were first prepared in tubes. The sequence of gRNA used for targeting around A165 is GAAGCTGGTTATCCACTGGG; and the sequence of gRNA used for targeting around C273 is CAGATGCATTTTAAC-CACAG. ssDNA sequence serving as template for HDR was added to the RNP and then transfected together into HepG2 cells. ssDNA of the template for *MTARC1* p.A165T KI: 5'- GGCTGTGACTTCAGGAAGCTGGTTATCCACTGGG CTGTGGCC TCGCCACAGTCCCTGCCCTCTATCTCCA GGC -3'; ssDNA of the template for *MTARC1* p.C273A KI: 5'- TGTCCCCCTTATGATGCTCTGTGTGTGTGTCC AGAGCCATTTTAACCACAGTGGACCCAGACACCGGTG TCATGAGCAGGAAGGAACC -3'. Three days after transfection, cells were plated into a 96-well plate at a density of 1 cell/well for generating single clonal cell lines. Each cell line was then screened for *MTARC1* genotype *via* PCR followed by Sanger sequencing. The sequencing result was analyzed using

the ICE online analysis tool on the Synthego website. For *MTARC1* p.A165T KI, cell lines with correct *MTARC1* p.A165T genotype were picked and expanded. A total of 14 cell lines were pooled together with the same cell number from each clonal line as a final pooled clonal HepG2 *MTARC1* p.A165T cell line used in this study. From the A165T KI experiment, cell lines with *MTARC1* WT genotype were also picked and expanded. A total of 31 cell lines were pooled together with same cell number from each clonal line as a final pooled clonal HepG2 WT cell line used in this study. The same procedure was followed to generate a final pooled clonal HepG2 *MTARC1* p.C273A KI cell line with a mixture of nine single clonal cell lines.

### Subcellular localization of *mARC1* protein in HepG2 cells

mARC1 WT, mARC1 A165T, and mARC1 C273A BacMam viruses were used to transduce HepG2 dKO cells in suspension ( $1.2 \times 10^5$  cells/ml) at a multiplicity of transduction of 7. After the addition of BacMam virus, cells were plated in collagen-coated, 96-well imaging plates (PerkinElmer 6055700) at  $1.2 \times 10^4$  cells/well in 100  $\mu$ l media and covered with Breathe-Easy seals (Sigma Z380059). The plates were incubated in a CO<sub>2</sub> incubator (37 °C, 5% CO<sub>2</sub>) overnight to allow for BacMam protein expression to occur.

On day 2, 100  $\mu$ l MitoTracker Deep Red (Invitrogen M22426, 100 nM, diluted in culture media) was added to each well of the 96-well plate. The plate was returned to the CO<sub>2</sub> incubator for 30 min. Medium in the plate was gently flicked off and the plate was washed 3 $\times$  with PBS. Cells in the plate were fixed in 3.7% formaldehyde for 20 min and then washed 3 $\times$  with PBS. The plate was then blocked with 50  $\mu$ l/well of PERM/BLOCK buffer (HBSS + 0.1% Triton X + 20 mM Hepes + 3% BSA) for 1.5 h on a slow shaker at room temperature. After the block buffer was gently flicked off, cells were then incubated with 50  $\mu$ l/well of 1  $\mu$ g/ml anti-mARC1 antibody (Sigma HPA028702, 1:100 dilution in PERM/BLOCK buffer) and placed on slow shaker overnight at 4 °C. Specificity of the anti-mARC1 antibody was validated using HepG2 mARC1 KO cell line.

On day 3, the cells were washed 2 $\times$  with wash buffer (HBSS + 0.1% Triton X + 20 mM Hepes). 50  $\mu$ l/well of 2  $\mu$ g/ml secondary goat anti-rabbit AF488 Ab (Invitrogen A32731, 1:1000 dilution in PERM/BLOCK buffer) was added to the plate. The plate was put on a slow shaker at RT for 1 h and then washed 2 $\times$  with wash buffer. Hoechst (Invitrogen H3570, 1:3000 in PBS) and Cell-Mask Orange (Invitrogen H32713, 1:20000 in PBS) stains were added to the cells for 30 min at RT in the dark. The plate was then washed twice with wash buffer. After the wash buffer was gently flicked off, 100  $\mu$ l of PBS was added to each well. Cells were then imaged with a PerkinElmer Opera Phenix automated confocal microscope using the 40 $\times$  water immersion objective. Images were imported to PerkinElmer Columbus 2.9.1 (<https://www.revity.com/product/image-data-storage-and-analysis-system-columbus>) image analysis software for quantification. FITC intensity of mARC1 protein for mitochondrial puncta and cytoplasm was quantitated for an average from over 6000 cells (6 wells, each well >1000 cells)



**PCR and ICE analysis for screening the clones with correct genotype**

PCR primers for sequence around mARC1 (A165) were as follows: forward primer: 5'-AAGCATAGCCAGGCC TGTG AATAA-3'; reverse primer: 5'-TGCAAAGTGTAAAAATTCT GGACT-3'. PCR primers for sequence around mARC1 (C273): forward primer: 5'- AATCTCATCTCAGGGGAATCAACT-3'; reverse primer: 5'- GTCACATCACTTCACTCCTACAC-3'. PCR primers for sequence for mARC2 KO: forward primer: 5'- CTGTCTGCCTGTCTTCTCCATTA-3', reverse primer: 5'- TGTCTATGTGTCAGGCCCAAAGT-3'. PCR products were generated using cell lysate for each cell line as template (DirectPCR lysis reagent, Viagen) and then purified by using QIAquick 96 PCR Purification Kit (Qiagen). The purified PCR products were sent to GENEWIZ for Sanger sequencing. The sequencing results were analyzed for genotype identification with DNASTAR Lasergene software (<https://www.dnastar.com/software/lasergene/>) and the Synthego ICE analysis tool.

**Simple Western (Jess) to detect protein expression**

The Jess system (ProteinSimple, capillary-based, instrument automated Western blotting) was used for protein detection. Cells on plates were harvested with TrypLE Select Enzyme (Gibco) and cell pellets were washed with PBS and then lysed with RIPA buffer (Thermo Fisher Scientific) + Protease Inhibitor (Cell Signaling Technology) + Benzoylase Nuclease (Sigma-Aldrich). Jess samples were prepared using the cell lysate following the protocol provided by ProteinSimple. The primary antibody used to detect mARC1 was from Abgent, and specificity of the antibody was validated using HepG2 mARC1 KO cell line. An antibody-targeting vinculin (Cell Signaling Technology) was always included in detection for each sample as an internal control. Signal area of the target protein provided by Jess was used for quantitative analysis of the protein amount in the sample. They were always normalized with the area of vinculin in the same sample and run in the same capillary.

**RT-qPCR to detect mRNA levels of mARC1 in various mARC1 KO & KI cells**

HepG2 with mARC1 WT, A165T, C273A and mARC1-KO pooled clonal cell lines were routinely cultured in T75 flasks. For RT-qPCR experiments,  $1 \times 10^6$  cells for each cell line were harvested. Following the protocol "TaqMan Gene Expression Cells-to-CT Kit" (Thermo Fisher Scientific), the samples were prepared for RT-qPCR assay. mARC1 assay (Thermo Fisher Scientific) with the probe targeting 3'-end of mRNA were used in the experiments.

**BAO substrate turnover assay**

HepG2 cells were cultured in 96-well plates with a density of  $5.0 \times 10^4$  cells/well. Twenty four hours later, cells were washed with HBSS (STEMCELL technologies) for 10 min. BAO (Sigma-Aldrich) in HBSS at various concentrations (2-fold series dilution starting from 1000  $\mu$ M) was added to corresponding wells. After cells were incubated with BAO for 3 h,

cell supernatant was harvested for detection of BAO/BA/3-fluoro-4-methylbenzamidine (employed as internal standard (IS)) using RF-QQQ-MS analysis method comprised of RF300 (Agilent Technologies) and Sciex 5000 or 5500 Mass Spectrometer (ABSciex). A graphite C18/type D solid phase extraction cartridge (Agilent Technologies) was used for analyte/IS adsorption/elution. The mobile phase A (for sample desalting) was composed of 0.5% (w/v) TFA in water. The mobile phase B (for elution) was composed of 0.5% TFA (w/v) in 20% (v/v) acetonitrile/water. Analyte detection was achieved by adsorption/elution: flow rate was 1.5 ml/min, 1.25 ml/min, and 1.00 ml/min for pump 1 (mobile phase A), pump 2 (mobile phase B), and pump 3 (mobile phase B), respectively. Multiple reaction monitoring methodology was used for BAO (Q1 137.0 Da/Q3: 121.0 Da), BA (Q1 121.0 Da/Q3 104.0 Da), and 3-fluoro-4-methylbenzamidine (Q1 153.0 Da/Q3 136.0 Da) detection.

**NOHA substrate turnover assay**

HepG2 cells were cultured in 96-well with a density of  $5.0 \times 10^4$  cells/well. Sixteen hours later, cells were washed with HBSS (STEMCELL technologies) for 10 min. NOHA (Sigma-Aldrich) in HBSS at various concentrations (2-fold series dilution starting from 250  $\mu$ M) was added to corresponding wells. After cells were incubated with NOHA for 3 h, cell supernatant was harvested for NOHA, L-arginine/<sup>13</sup>C<sub>6</sub>-L-arginine (L-Arg IS), and L-citrulline/<sup>2</sup>H<sub>4</sub>-L-citrulline (L-Cit IS) RF-QQQ-MS detection using RF-QQQ-MS analysis (Sciex 5000/5500 Mass Spectrometry). Solid phase extraction/mobile phase A/B conditions were the same as those used in the BAO substrate turnover assay. MRM methodology was used for NOHA (Q1 191.1 Da/Q3 146.0 Da), L-Arg (Q1 175.1 Da/Q3 116.0 Da), <sup>13</sup>C<sub>6</sub>-L-Arg (Q1 181.1 Da/Q3 121.0 Da), L-Cit (Q1 176.2 Da/Q3 159.0 Da), and <sup>2</sup>H<sub>4</sub>-L-Cit (Q1 180.2 Da/Q3 163.0 Da) detection.

**mARC1 protein stability test in HepG2 cells**

HepG2 cells expressing different forms of mARC1 (WT, A165T, or C273A) were seeded on 96-well plates with a density of  $6.0 \times 10^4$  cells/well in 200  $\mu$ l culture medium and incubated at 37 °C in a 5% CO<sub>2</sub> incubator for 16 h. A final concentration of 0  $\mu$ M (DMSO only), 10  $\mu$ M, or 20  $\mu$ M of cycloheximide (dissolved in DMSO) was added to different wells of each cell line in culture medium (0.0067% DMSO in all wells). After the cells were incubated with cycloheximide for 8 h, they were then harvested and pelleted. Cell lysates were prepared from the cell pellets and run on ProteinSimple Jess for mARC1 protein detection.

**mARC1 protein immunoprecipitation and ubiquitinated mARC1 protein detection**

HepG2 dKO cells were seeded on T150 plates at a density of  $1.84 \times 10^7$  cells/flask together with one of the BacMam viruses expressing either C-terminal Flag-tagged mARC1 WT, A165T, or C273A at a multiplicity of transduction of 1, respectively. Three flasks were prepared for each cell line. Cells were

## Characterization of mARC1 p.A165T variant

incubated in a CO<sub>2</sub> incubator for 16 h. DMSO or cycloheximide (dissolved in DMSO) were added to different flasks with each BacMam virus to achieve a final concentration of 0 μM (DMSO) (1 flask) or 20 μM cycloheximide (2 flasks) in culture medium and incubated with cells for 8 h. DMSO or MG-132 was then added to the cells to achieve a final concentration of 0 μM (DMSO) or 0.6 μM MG-132 (1 of the 2 flasks with 20 μM cycloheximide) and incubated with the cells for 2 h. A total of three conditions were prepared for cells with each BacMam virus: 0 μM cycloheximide + 0 μM MG-132, 20 μM cycloheximide + 0 μM MG-132, and 20 μM cycloheximide + 0.6 μM MG-132. Cells were then harvested and lysed for immunoprecipitation with Pierce Anti-DYKDDDDK Magnetic Agarose (Invitrogen). For the eluate from the IP, ubiquitinated mARC1 protein was detected with rabbit anti-ubiquitin antibody (Cell Signaling Technology). mARC1 protein pulled down by IP was also detected with anti-mARC1 antibody (Abgent). Protein bands in the image data were quantitated by ImageJ application. Relative amount of ubiquitinated mARC1 protein was normalized by non-ubiquitinated mARC1 protein immunoprecipitated.

### Statistical analysis for all experiments

GraphPad Prism 9 was used for statistical analysis. Four replicates for each condition were performed and outliers were removed if identified (Grubbs' test,  $p < 0.05$ ). Data comparison was analyzed using unpaired  $t$  test.

### Data availability

All data are contained in this article.

**Supporting information**—This article contains supporting information.

**Acknowledgments**—We thank the project team for their kind support and helpful discussion and Mark Harpel for his careful reviews and insightful suggestions.

**Author contributions**—W. H., C. W., T. C., G. J. G., and T. A. D. conceptualization; W. H., C. W., and T. C. data curation; W. H., C. W., and T. C. formal analysis; W. H., C. W., and T. C. investigation; W. H., C. W., T. C., and M. N. B. methodology; W. H., C. W., T. C., and M. N. B. validation; W. H., C. W., and T. C. visualization; W. H. writing—original draft; W. H., J. J. B., Q. L., G. J. G., and T. A. D. writing—review and editing; M. N. B., J. J. B., and G. J. G. resources; J. J. B. and G. J. G. project administration; J. J. B., Q. L., G. J. G., and T. A. D. supervision.

**Conflict of interest**—The authors declare that they have no conflicts of interest with the contents of this article.

**Abbreviations**—The abbreviations used are: BA, benzamidine; BAO, benzamidoxime; CYB5B, cytochrome *b*<sub>5</sub> type B; CYB5R3, NADH-cytochrome *b*<sub>5</sub> reductase; dKO, double knockout; gRNA, guide RNA; GWAS, genome-wide association studies; ICE, Inference of CRISPR Edits; IP, immunoprecipitation; IP'd, immunoprecipitated; IS, internal standard; KI, knock-in; mARC1, mitochondrial amidoxime-reducing component 1; Mo, molybdenum; Moco, Mo

cofactor; *MTARC1*, Mitochondrial amidoxime-reducing component 1; NAFLD, nonalcoholic fatty liver disease; NOHA, N<sup>ω</sup>-hydroxy-L-arginine; RF-QQQ-MS, RapidFire-Triple Quadrupole-Mass Spectrometry; RNP, ribonucleoprotein.

### References

- Schneider, C. V., Schneider, K. M., Conlon, D. M., Park, J., Vujkovic, M., Zandvakili, I., *et al.* (2021) A genome-first approach to mortality and metabolic phenotypes in *MTARC1* p.Ala165Thr (rs2642438) heterozygotes and homozygotes. *Med (N Y)* **2**, 851–863 e853
- Younossi, Z. M., Blissett, D., Blissett, R., Henry, L., Stepanova, M., Younossi, Y., *et al.* (2016) The economic and clinical burden of nonalcoholic fatty liver disease in the United States and Europe. *Hepatology* **64**, 1577–1586
- Romeo, S. (2020) *MARC1* and *HNRNPUL1*: two novel Players in alcohol-related liver disease. *Gastroenterology* **159**, 1231–1232
- Wree, A., Broderick, L., Canbay, A., Hoffman, H. M., and Feldstein, A. E. (2013) From NAFLD to NASH to cirrhosis—new insights into disease mechanisms. *Nat. Rev. Gastroenterol. Hepatol.* **10**, 627–636
- Salt, W. B., 2nd (2004) Nonalcoholic fatty liver disease (NAFLD): a comprehensive review. *J. Insur. Med.* **36**, 27–41
- Tapner, E. B., and Parikh, N. D. (2018) Mortality due to cirrhosis and liver cancer in the United States, 1999–2016: observational study. *BMJ* **362**, k2817
- Asrani, S. K., Devarbhavi, H., Eaton, J., and Kamath, P. S. (2019) Burden of liver diseases in the world. *J. Hepatol.* **70**, 151–171
- Dufour, J. F., Caussy, C., and Loomba, R. (2020) Combination therapy for non-alcoholic steatohepatitis: rationale, opportunities and challenges. *Gut* **69**, 1877–1884
- King, E. A., Davis, J. W., and Degner, J. F. (2019) Are drug targets with genetic support twice as likely to be approved? Revised estimates of the impact of genetic support for drug mechanisms on the probability of drug approval. *PLoS Genet.* **15**, e1008489
- Emdin, C. A., Haas, M. E., Khera, A. V., Aragam, K., Chaffin, M., Klarin, D., *et al.* (2020) A missense variant in Mitochondrial Amidoxime Reducing Component 1 gene and protection against liver disease. *PLoS Genet.* **16**, e1008629
- Innes, H., Buch, S., Hutchinson, S., Guha, I. N., Morling, J. R., Barnes, E., *et al.* (2020) Genome-wide association study for alcohol-related cirrhosis identifies risk loci in *MARC1* and *HNRNPUL1*. *Gastroenterology* **159**, 1276–1289 e1277
- Luukkonen, P. K., Juuti, A., Sammalkorpi, H., Penttila, A. K., Oresic, M., Hyotylainen, T., *et al.* (2020) *MARC1* variant rs2642438 increases hepatic phosphatidylcholines and decreases severity of non-alcoholic fatty liver disease in humans. *J. Hepatol.* **73**, 725–726
- Hudert, C. A., Adams, L. A., Alisi, A., Anstee, Q. M., Crudele, A., Draijer, L. G., *et al.* (2022) Variants in mitochondrial amidoxime reducing component 1 and hydroxysteroid 17-beta dehydrogenase 13 reduce severity of nonalcoholic fatty liver disease in children and suppress fibrotic pathways through distinct mechanisms. *Hepatol. Commun.* **6**, 1934–1948
- Havemeyer, A., Bittner, F., Wollers, S., Mendel, R., Kunze, T., and Clement, B. (2006) Identification of the missing component in the mitochondrial benzamidoxime prodrug-converting system as a novel molybdenum enzyme. *J. Biol. Chem.* **281**, 34796–34802
- Klein, J. M., Busch, J. D., Potting, C., Baker, M. J., Langer, T., and Schwarz, G. (2012) The mitochondrial amidoxime-reducing component (mARC1) is a novel signal-anchored protein of the outer mitochondrial membrane. *J. Biol. Chem.* **287**, 42795–42803
- Andersson, S., Hofmann, Y., Nordling, A., Li, X. Q., Nivelius, S., Andersson, T. B., *et al.* (2005) Characterization and partial purification of the rat and human enzyme systems active in the reduction of N-hydroxymelagatran and benzamidoxime. *Drug Metab. Dispos.* **33**, 570–578
- Ott, G., Plitzko, B., Krischkowski, C., Reichmann, D., Bittner, F., Mendel, R. R., *et al.* (2014) Reduction of sulfamethoxazole hydroxylamine (SMX-

- HA) by the mitochondrial amidoxime reducing component (mARC). *Chem. Res. Toxicol.* **27**, 1687–1695
18. Indorf, P., Kubitzka, C., Scheidig, A. J., Kunze, T., and Clement, B. (2020) Drug metabolism by the mitochondrial amidoxime reducing component (mARC): rapid assay and identification of new substrates. *J. Med. Chem.* **63**, 6538–6546
  19. Plitzko, B., Havemeyer, A., Kunze, T., and Clement, B. (2015) The pivotal role of the mitochondrial amidoxime reducing component 2 in protecting human cells against apoptotic effects of the base analog N6-hydroxylaminopurine. *J. Biol. Chem.* **290**, 10126–10135
  20. Kotthaus, J., Wahl, B., Havemeyer, A., Kotthaus, J., Schade, D., Garbe-Schonberg, D., et al. (2011) Reduction of N(omega)-hydroxy-L-arginine by the mitochondrial amidoxime reducing component (mARC). *Biochem. J.* **433**, 383–391
  21. Plitzko, B., Ott, G., Reichmann, D., Henderson, C. J., Wolf, C. R., Mendel, R., et al. (2013) The involvement of mitochondrial amidoxime reducing components 1 and 2 and mitochondrial cytochrome b5 in N-reductive metabolism in human cells. *J. Biol. Chem.* **288**, 20228–20237
  22. Neve, E. P., Nordling, A., Andersson, T. B., Hellman, U., Diczfalusy, U., Johansson, I., et al. (2012) Amidoxime reductase system containing cytochrome b5 type B (CYB5B) and MOSC2 is of importance for lipid synthesis in adipocyte mitochondria. *J. Biol. Chem.* **287**, 6307–6317
  23. Jakobs, H. H., Froriep, D., Havemeyer, A., Mendel, R. R., Bittner, F., and Clement, B. (2014) The mitochondrial amidoxime reducing component (mARC): involvement in metabolic reduction of N-oxides, oximes and N-hydroxyamidinohydrazones. *ChemMedChem* **9**, 2381–2387
  24. Jakobs, H. H., Mikula, M., Havemeyer, A., Strzalkowska, A., Borowa-Chmielak, M., Dzwonek, A., et al. (2014) The N-reductive system composed of mitochondrial amidoxime reducing component (mARC), cytochrome b5 (CYB5B) and cytochrome b5 reductase (CYB5R) is regulated by fasting and high fat diet in mice. *PLoS One* **9**, e105371
  25. Zelickson, B. R., Benavides, G. A., Johnson, M. S., Chacko, B. K., Venkatraman, A., Landar, A., et al. (2011) Nitric oxide and hypoxia exacerbate alcohol-induced mitochondrial dysfunction in hepatocytes. *Biochim. Biophys. Acta* **1807**, 1573–1582
  26. Brown, G. C. (2007) Nitric oxide and mitochondria. *Front Biosci.* **12**, 1024–1033
  27. Duvigneau, J. C., and Kozlov, A. V. (2017) Pathological impact of the interaction of NO and CO with mitochondria in critical care diseases. *Front Med. (Lausanne)* **4**, 223
  28. Dai, L., Brookes, P. S., Darley-Usmar, V. M., and Anderson, P. G. (2001) Bioenergetics in cardiac hypertrophy: mitochondrial respiration as a pathological target of NO<sup>•</sup>. *Am. J. Physiol. Heart Circ. Physiol.* **281**, H2261–H2269
  29. Pessayre, D., and Fromenty, B. (2005) NASH: a mitochondrial disease. *J. Hepatol.* **42**, 928–940
  30. Ott, G., Reichmann, D., Boerger, C., Cascorbi, I., Bittner, F., Mendel, R. R., et al. (2014) Functional characterization of protein variants encoded by nonsynonymous single nucleotide polymorphisms in MARC1 and MARC2 in healthy Caucasians. *Drug Metab. Dispos.* **42**, 718–725
  31. Chen, S., Francioli, L. C., Goodrich, J. K., Collins, R. L., Kanai, M., Wang, Q., et al. (2024) A genomic mutational constraint map using variation in 76,156 human genomes. *Nature* **625**, 92–100
  32. Sparacino-Watkins, C. E., Tejero, J., Sun, B., Gauthier, M. C., Thomas, J., Ragireddy, V., et al. (2014) Nitrite reductase and nitric-oxide synthase activity of the mitochondrial molybdopterin enzymes mARC1 and mARC2. *J. Biol. Chem.* **289**, 10345–10358
  33. Kubitzka, C., Bittner, F., Ginsel, C., Havemeyer, A., Clement, B., and Scheidig, A. J. (2018) Crystal structure of human mARC1 reveals its exceptional position among eukaryotic molybdenum enzymes. *Proc. Natl. Acad. Sci. U. S. A.* **115**, 11958–11963
  34. Mathieson, T., Franken, H., Kosinski, J., Kurzawa, N., Zinn, N., Sweetman, G., et al. (2018) Systematic analysis of protein turnover in primary cells. *Nat. Commun.* **9**, 689
  35. Lewis, L. C., Chen, L., Hameed, L. S., Kitchen, R. R., Maroteau, C., Nagarajan, S. R., et al. (2023) Hepatocyte mARC1 promotes fatty liver disease. *JHEP Rep.* **5**, 100693
  36. Krompholz, N., Krischkowski, C., Reichmann, D., Garbe-Schonberg, D., Mendel, R. R., Bittner, F., et al. (2012) The mitochondrial Amidoxime Reducing Component (mARC) is involved in detoxification of N-hydroxylated base analogues. *Chem. Res. Toxicol.* **25**, 2443–2450
  37. Buch, S., Stickel, F., Trepo, E., Way, M., Herrmann, A., Nischalke, H. D., et al. (2015) A genome-wide association study confirms PNPLA3 and identifies TM6SF2 and MBOAT7 as risk loci for alcohol-related cirrhosis. *Nat. Genet.* **47**, 1443–1448
  38. Abul-Husn, N. S., Cheng, X., Li, A. H., Xin, Y., Schurmann, C., Stevis, P., et al. (2018) A protein-truncating HSD17B13 variant and protection from chronic liver disease. *N. Engl. J. Med.* **378**, 1096–1106
  39. Romeo, S., Kozlitina, J., Xing, C., Pertsemlidis, A., Cox, D., Pennacchio, L. A., et al. (2008) Genetic variation in PNPLA3 confers susceptibility to nonalcoholic fatty liver disease. *Nat. Genet.* **40**, 1461–1465
  40. Stickel, F., Lutz, P., Buch, S., Nischalke, H. D., Silva, I., Rausch, V., et al. (2020) Genetic variation in HSD17B13 reduces the risk of developing cirrhosis and hepatocellular carcinoma in alcohol misusers. *Hepatology* **72**, 88–102
  41. Smagris, E., Shihanian, L. M., Mintah, I. J., Bigdelou, P., Livson, Y., Brown, H., et al. (2024) Divergent role of mitochondrial amidoxime reducing component 1 (MARC1) in human and mouse. *PLoS Genet.* **20**, e1011179
  42. Wahl, B., Reichmann, D., Niks, D., Krompholz, N., Havemeyer, A., Clement, B., et al. (2010) Biochemical and spectroscopic characterization of the human mitochondrial amidoxime reducing components hmARC-1 and hmARC-2 suggests the existence of a new molybdenum enzyme family in eukaryotes. *J. Biol. Chem.* **285**, 37847–37859
  43. Bentebbal, S. A., Meqbel, B. R., Salter, A., Allan, V., Burke, B., and Horn, H. F. (2021) A human infertility-associated KASH5 variant promotes mitochondrial localization. *Sci. Rep.* **11**, 10133
  44. Struwe, M. A., Clement, B., and Scheidig, A. J. (2022) Letter to the editor: The clinically relevant MTARC1 p.Ala165Thr variant impacts neither the fold nor active site architecture of the human mARC1 protein. *Hepatol. Commun.* **6**, 3277–3278
  45. Vitali, D. G., Sinzel, M., Bulthuis, E. P., Kolb, A., Zabel, S., Mehlhorn, D. G., et al. (2018) The GET pathway can increase the risk of mitochondrial outer membrane proteins to be mistargeted to the ER. *J. Cell Sci.* **131**, jcs211110
  46. Sulkshane, P., Ram, J., and Glickman, M. H. (2020) Ubiquitination of intramitochondrial proteins: implications for metabolic adaptability. *Biomolecules* **10**, 1559
  47. Karbowski, M., and Youle, R. J. (2011) Regulating mitochondrial outer membrane proteins by ubiquitination and proteasomal degradation. *Curr. Opin. Cell Biol.* **23**, 476–482
  48. Nakatsukasa, K., Huyer, G., Michaelis, S., and Brodsky, J. L. (2008) Dissecting the ER-associated degradation of a misfolded polytopic membrane protein. *Cell* **132**, 101–112
  49. Tai, H. C., and Schuman, E. M. (2008) Ubiquitin, the proteasome and protein degradation in neuronal function and dysfunction. *Nat. Rev. Neurosci.* **9**, 826–838
  50. Wu, M., Tie, M., Hu, L., Yang, Y., Chen, Y., Ferguson, D., et al. (2024) Fatty liver disease protective MTARC1 p.A165T variant reduces the protein stability of MTARC1. *Biochem. Biophys. Res. Commun.* **702**, 149655
  51. Dutta, T., Sasidharan, K., Ciociola, E., Pennisi, G., Noto, F. R., Kovooru, L., et al. (2024) Mitochondrial amidoxime-reducing component 1 p. Ala165Thr increases protein degradation mediated by the proteasome. *Liver Int.* **44**, 1219–1232
  52. Fornwald, J. A., Lu, Q., Boyce, F. M., and Ames, R. S. (2016) Gene expression in mammalian cells using BacMam, a modified baculovirus system. *Methods Mol. Biol.* **1350**, 95–116